Effect of sensor position on the performance of CO_2–based demand controlled ventilation

Gen Pei[1], Donghyun Rim[1*], Stefano Schiavon[2], Matthew Vannucci[2]

[1]Department of Architectural Engineering, Pennsylvania State University, University Park, PA, USA

[2]Center for the Built Environment, University of California Berkeley, CA, USA

Abstract

CO_2–based demand controlled ventilation (DCV) can save energy while maintaining acceptable indoor air quality. CO_2 concentration may vary within an occupied space and it is unclear how sensor location influences the ventilation and energy performances. The objective of the present study is to investigate the effect of CO_2 sensor position on the performance of DCV systems under mixing and displacement ventilation. Experimentally validated computational fluid dynamics (CFD) models were simulated under representative indoor ventilation and occupancy conditions. The results show that the ventilation strategy, occupancy level, and air change rate have notable impacts on the CO_2 sensing performance. Under mixing ventilation, CO_2 sensors placed at the room exhaust can meet the requirements of sensor accuracy defined by ASTM E741 and California Title 24. However, the sensor errors associated with sensor location can be higher than the acceptable threshold under displacement ventilation, which exhibits vertical CO_2 stratification with two separated zones (lower transition zone and upper uniform zone). The dividing height of the two zones is highly sensitive to the occupancy level. In such cases, exhaust sensors can overestimate the breathing zone concentration and result in additional energy consumptions for thermal conditioning as well as fan operation, especially for densely occupied buildings. The study findings suggest that for ensuring good performance of CO_2–based displacement ventilation, it is necessary to develop quantitative relationships between CO_2 concentrations at the breathing height and the room exhaust considering ventilation strategies.

Keywords: indoor air quality; CO_2 sensing; computational fluid dynamics; building energy; displacement ventilation

Highlights

- CO_2 sensors near occupants result in large errors under displacement ventilation
- CO_2 sensors at breathing height perform well for constant occupancy conditions
- CO_2 sensors at breathing height yield errors with varying occupancy
- Under mixing ventilation, CO_2 sensors at the room exhaust yield a good accuracy

https://doi.org/10.1016/j.enbuild.2019.109358
escholarship.org/uc/item/8n23p8c4

Graphical abstract

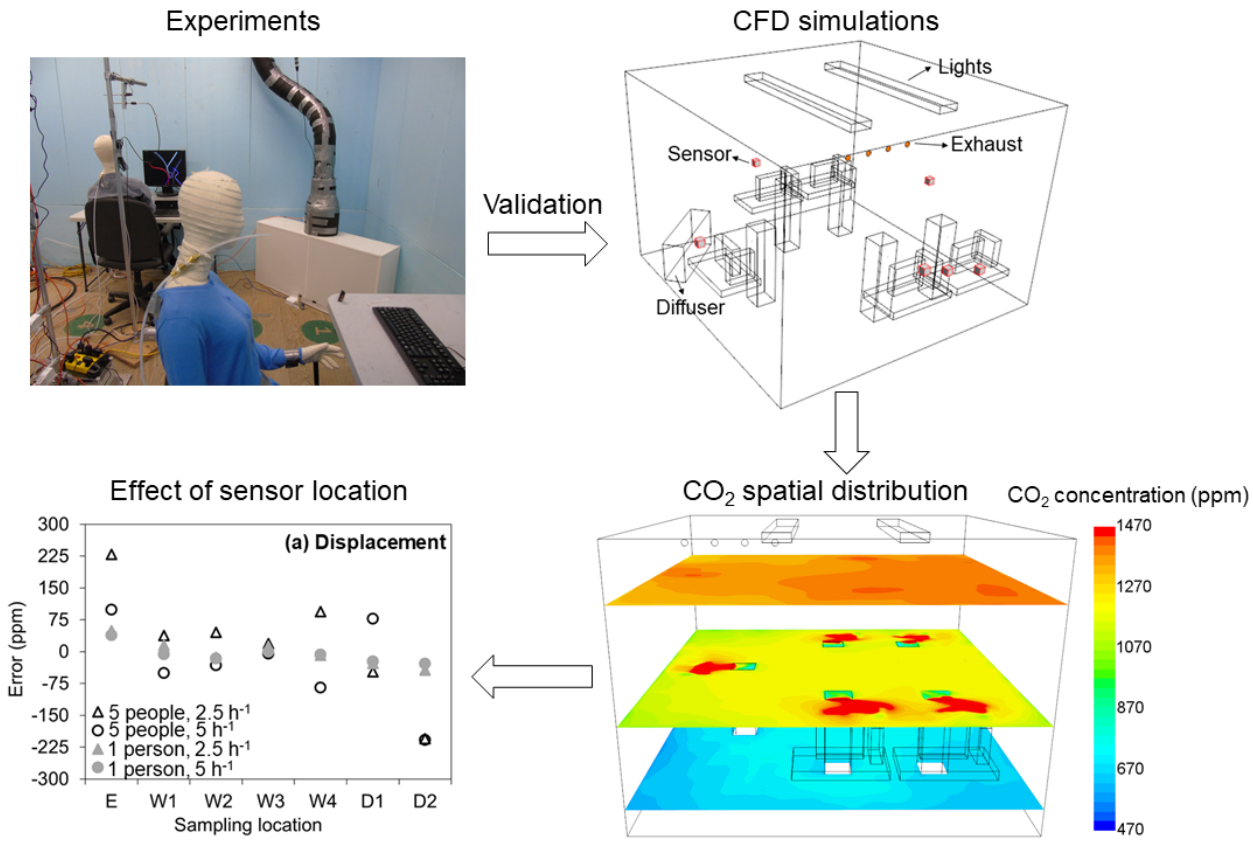

https://doi.org/10.1016/j.enbuild.2019.109358
escholarship.org/uc/item/8n23p8c4

Nomenclature

Symbols			
a	fan power coefficient (–)	P_f	fan power (kW)
C(t)	exhaust CO_2 concentration (ppm)	Q	outdoor air volumetric flow rate (m^3/h)
C_{in}	equilibrium CO_2 concentration in the space (ppm)	q	total heat load (kW)
$\mathbf{C_{out}}$	outdoor CO_2 concentration (ppm)	T_e	air temperature at the room exhaust (°C)
c_p	air specific heat (kJ/(kg·K))	T_s	supply air temperature (°C)
D_{eff}	effective diffusion coefficient (–)	t	time (s)
G	CO_2 generation rate (m^3/h)	t_S	solution time (h)
h_1	specific enthalpy of outdoor air (kJ/kg)	u	fluid velocity vector (m/s)
h_2	specific enthalpy of air that leaves coil (kJ/kg)	Y_{CO_2}	mass fraction of CO_2 (–)
j_{CO_2}	mass flux of CO_2 (kg/s)	ρ	density of fluid (kg/m^3)
n	number of rooms (–)	λ	air change rate (h^{-1})

https://doi.org/10.1016/j.enbuild.2019.109358
escholarship.org/uc/item/8n23p8c4

1. Introduction

In an occupied space, it is necessary to control the indoor pollutant concentrations by providing adequate outdoor fresh air to the space. Insufficient ventilation in an occupied room has implications in comfort, productivity, and health [1-3]. However, at the same time, a significant amount of energy can be used for providing thermally conditioned outdoor air to an occupied space [4-6]. Considering this challenge, demand-controlled ventilation (DCV) has been used to adjust ventilation rates based on the occupancy level, thereby conserving ventilation energy while maintaining acceptable indoor air quality [7].

Several previous studies evaluated the performance of DCV in different types of occupied spaces and reported that a well–designed DCV can save energy for thermal conditioning and fan operation without compromising indoor air quality [8-14]. For instance, Fisk and Almeida [12] reviewed case studies of DCV applied to various types of buildings and reported notable energy saving with a payback period typically of a few years. Budaiwi and AlHomoud [8] used theoretical models to examine the effects of different ventilation strategies on indoor air quality and cooling energy consumption for a single-zone enclosure with a design occupant density of 10 people/100 m^2. They reported that with DCV, more than 50 % cooling energy could be saved while maintaining pollutant concentrations below the recommended level. Schibuola et al. [10] analyzed the performance of a DCV system in a university library with a design occupancy of 20 people/100 m^2 using measurement data from a supervisory system and revealed that the DCV system yielded 22% thermal conditioning energy saving and 40% fan energy saving.

Indoor CO_2 concentrations can be monitored in buildings for the evaluation of ventilation and air quality control [2,15]. As humans are the main CO_2 emission sources in most occupied buildings, indoor CO_2 concentration has been a proxy indicator of bioeffluents from humans [7,16]. The difference between indoor and outdoor CO_2 concentrations can be used to estimate the ventilation rate [16,17]. Several standards have defined the allowable level for the indoor CO_2 concentration to maintain the acceptable indoor air quality. ANSI/ASHRAE Standard 62.1 [18] states that maintaining CO_2 concentration in a space no greater than 700 ppm above outdoor air levels can meet the standard requirements. ASTM Standard D6245 [16] suggests maintaining CO_2 concentrations within 650 ppm above outdoors can maintain body odor below an acceptable level.

To control indoor CO_2 concentrations, there are mainly three conventional control methods used for CO_2–based DCV systems: 1) set point control, 2) proportional control, and 3) exponential control. Set point control is an on–off ventilation strategy based on a specific CO_2 setpoint. This approach has limited applications due to a relatively long response time. It is more typical to use proportional or exponential modulation of outdoor air flow rate based on the time variation of the indoor CO_2 concentration [19]. However, all these methods are operated under the assumption of steady–state condition that may hardly be reached in practice. For this situation, previous studies developed a control strategy that calculates supply outdoor air flow rates dynamically by solving the transient CO_2 mass balance equation and maintain indoor CO_2 concentration near the setpoint [20,21]. CO_2 concentrations within the occupant breathing zone provide a good basis for

estimating ventilation rates required for a given space. However, an inappropriate CO_2 sensor arrangement may lead to wrong representation of the breathing zone concentration. Previous studies reported non-uniform spatial distributions of CO_2 in occupied spaces under different ventilation conditions [22-29]. Experiments conducted by Stymne et al. [23] reported a vertical gradient of CO_2 concentration in rooms with displacement ventilation. The concentrations relative to exhaust concentration varied from 20% to 120% within 2 m height. The non–uniform CO_2 distribution may occur in mixing ventilation systems with relatively small air flow rates. For example, Mahyuddin and Awbi [25] reported 94 ppm CO_2 concentration variation in an 18 m^3 experimental chamber under mixing ventilation with a supply air flow rate of 4 L/s. Bulińska et al. [28] performed experimentally validated numerical simulations to predict the spread of CO_2 in a naturally ventilated bedroom, and reported that the CO_2 concentrations in the vicinity of occupants, window, and heat sources could be more than 10% higher or lower than the room average.

Even with possible non-uniform CO_2 distribution in occupied spaces, an extensive review study by Mahyuddin and Awbi [26] showed that most building designers prefer to place only one CO_2 sensor at a representative position in an occupied space. Meanwhile, several other studies have explored heterogeneous indoor pollutant distributions due to building operating parameters such as ventilation strategy and occupant density [30,31]. For example, Rim and Novoselac [30] examined the dispersion of a tracer gas (SF_6, sulfur hexafluoride) in two different airflow regimes: mixing flow and buoyancy–driven flow. They found that the temporal and spatial variations of SF_6 concentration were larger in the buoyancy–driven flow regime. Maldonado and Woods [31] summarized three main factors that affects the indoor contaminant distributions: (1) the location and strength of the pollutant source, (2) the internal air movements as well as (3) the type and location of the supply air diffusers. However, very few studies in the literature examined the effect of CO_2 sensor position on the performance of DCV systems, considering building operating and occupancy conditions. Based on this background, the primary objective of present study is to examine (1) spatial distribution of CO_2 in occupied spaces influenced by ventilation strategy, air change rate, and occupancy level; and (2) evaluate the impacts of sensor positioning on estimating breathing zone CO_2 concentration and performance of a DCV system.

2. Methods

In the present study, we employed the Computational Fluid Dynamics (CFD) model and validation experiments to simulate the dispersion of CO_2 in a mechanically ventilated room. The following section presents the CFD model validation experiments, description of the applied CFD model, and parametric analysis.

2.1 Validation of CFD model

Based on the previous studies and recommendations regarding CFD validation process [32-36], we performed experiments in a full-scale environmental chamber and used the measurement data for validating the CFD model as described in the following sections.

2.1.1 Experimental set–up

We conducted full–scale experiments in a 4.27 × 4.27 × 3 m (length × width × height) environmental chamber to simulate a typical private or shared office (see Figure 1). A detail description of the room was reported in the study of Schiavon et al. [37]. We performed five validation experiment with various number of manikins and air flow rates (see Table 1). The heat sources included five heated manikins (B, C, D, E at 85 W and A at 65 W), five desktop computers (the heat from each computer ranged from 60 to 134 W), lightings (190 W) and other instruments (13 W). Figure 1a shows the test chamber layout with the locations of the manikins. Table 1 summaries the total heat load and load per unit area for each case. Supply air was provided at temperature of 18 °C using a low momentum displacement diffuser (1.215 × 0.615 m) at the floor level. Room air was exhausted through four outlets at the ceiling level. The climatic chamber meets the requirements by DIN EN 14240-2004 [38] for the room dimensions and manikin setup. During the experiment, CO_2 was continuously released from a tube with a 4.57 mm diameter in front of the nose of manikin (see Figure 1b) to simulate the CO_2 emission from breathing. CO_2 was released at room temperature (25 °C), which was lower than the actual temperature of exhaled air by a person performing office task. Nevertheless, Srebric and Chen [39] suggested the additional thermal energy of exhaled CO_2 is relatively small and negligible in the experimental validation of indoor environment CFD model. The CO_2 emission rate was 0.0072 L/s for each manikin, which was 13% higher than the empirical CO_2 generation rate of male performing office work (0.0064 L/s) [40]. This higher release rate was used to maximize the accuracy of the experimental tests and had little effect on the CFD validation process.

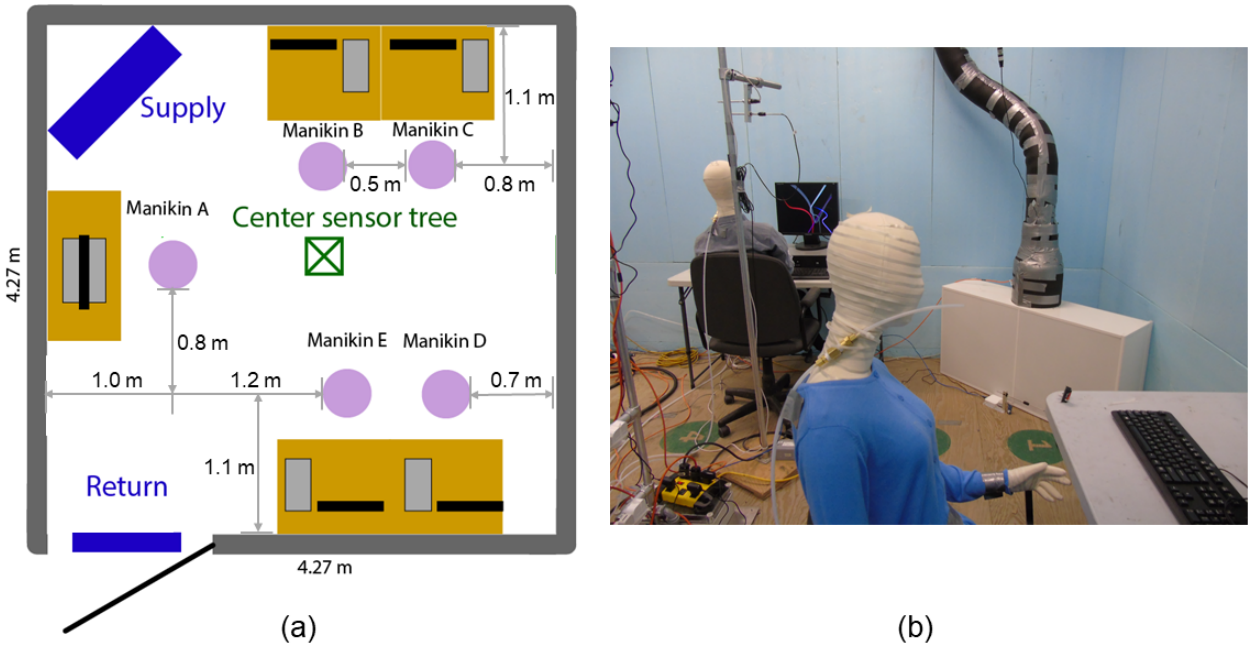

Figure 1. (a) A schematic of the experiment set–up; (b) a picture of the chamber test.

We measured the vertical CO_2 concentration profile at the center of the chamber (see Figure 1a). Along this sampling line, six CO_2 sensors were placed at heights of 0.3, 0.6, 1.1, 1.7, 2.2, 2.6 m. Note that the accuracy of CO_2 sensor was ±25 ppm or ± 3% of reading for the detection range of 400-2000 ppm.

Table 1. Parameters and comparison results for five validation cases**.**

Case	Manikins turned on	Total heat load (W)	Load per unit area (W/m²)	Airflow rate (L/s·person)	Inlet air velocity (m/s)	Sensor error (ppm)	MAE (ppm)
1	D	422	23	36	0.05	44	58
2	A,C,D	765	42	20	0.08	45	93
3	A,C,D	765	42	40	0.16	46	59
4	A,B,C,D,E	1076	59	20	0.13	48	86
5	A,B,C,D,E	1076	59	34	0.22	43	55

2.1.2 Description of CFD model

We established three–dimensional geometry models based on the set–up of the environmental chamber with one, three and five occupants respectively, as discussed in Section 2.1.1 (see Figure 3a). The only difference was the shape of the thermal manikin simplified to a rectangular solid. The simplified manikin geometry only affected the airflow in the vicinity of manikin, but simulated the overall airflow with reasonable accuracy while saving computation time [41-42].

We discretized the computational model using polyhedral mesh considering its potential to provide good calculation accuracy with a reduced computational load [43]. We refined computational meshes in the proximity of the heat sources (i.e., manikin, computer and lights), the air inlet and outlet, and the CO_2 inlet to accurately capture the heat and mass transfers in the grid–sensitive regions (see Figure 3b). The total numbers of the grid cells for the simulation domain with one, three and five occupants were approximately 170,000, 280,000 and 400,000, respectively.

We used a CFD solver Star-CCM+ [44] to compute the indoor airflow and CO_2 transport in the space. The solver employed the Reynolds Averaged Navier–Stokes (RANS) equations with the two–equation Shear Stress Transport (SST) k–ω turbulence model. The SST k–ω turbulence model combines the advantages of both k–ε and k–ω models and shows good performance in predicting stratified indoor airflow associated with thermal plumes [45-47]. We performed the unsteady simulations to calculate time–varying CO_2 concentrations for a period of two hours with a time step of 1 s.

https://doi.org/10.1016/j.enbuild.2019.109358
escholarship.org/uc/item/8n23p8c4

We used three dimensional convection–diffusion equations to simulate the transport of CO_2 [48-49]:

$$\frac{\partial(\rho Y_{CO_2})}{\partial t} + \nabla\cdot(\rho Y_{CO_2} u) = -\nabla\cdot j_{CO_2} \quad (1)$$

where ρ is the density of fluid (kg/m^3), t is the time (s), u is the fluid velocity vector (m/s), Y_{CO_2} is the mass fraction of CO_2 and j_{CO_2} is the mass flux of CO_2 (kg/s) that can be calculated as follows:

$$j_{CO_2} = -D_{eff}\nabla\cdot Y_{CO_2} \quad (2)$$

where D_{eff} is the effective diffusion coefficient that includes molecular and turbulent diffusion.

The boundary conditions applied in the CFD model were based on the experimental parameters described in Section 2.1.1, including the supply air conditions, CO_2 emission conditions and heat fluxes from indoor heat sources. The supply air inlet velocity varied with ventilation rate for each case (see Table 1). The CO_2 was released using a boundary condition of velocity inlet at the velocity magnitude of 0.45 m/s and the emission rate of 0.0072 L/s for each manikin. Note that all indoor heat fluxes were divided into convective and radiative portions based on ASHRAE Handbooks of Fundaments [50]. The radiative and convective portions were set to 58% and 42% for occupant, 40% and 60% for monitor, 10% and 90% for computer as well as 67% and 33% for lights. The convective heat fluxes were applied to the heat source surfaces while radiative heat loads were distributed to the surrounding wall surfaces.

2.1.2 Validation process

Figure 2 compares the simulated and measured vertical CO_2 profiles at the center of the room for the five validation cases. The simulated CO_2 concentration is the average of steady−state concentrations at 27 sampling points covering a 0.05 m^3 of air volume around the actual sensor position to reduce the possible simulation uncertainty with a point sampling. The error bars represent the standard deviations of concentrations at these 27 points for simulation results and the sensor errors for the measurements. Figure 2 demonstrates vertical CO_2 stratification in the displacement ventilation due to the buoyancy–driven airflow. The simulation results do not perfectly agree with the measurements, which is mainly due to the simplified geometry of the thermal manikin. However, the simulation and measurement results show a similar trend of vertical CO_2 profile. For each validation test, the mean absolute error (MAE) was calculated as the average of the absolute differences between the measured and simulated steady-state CO2 concentrations at six sensor locations (see Table 1). Relatively larger MAEs are observed in cases 2 and 4 (93 and 86 ppm). In such cases, ventilation rates are relatively low and the

concentrations appear to be very sensitive to the buoyancy driven flow with the simplified occupant geometry as well as sampling locations, especially at the levels of occupant's upper body and head [51]. Although the simulation results and measurements do not perfectly match, the differences between MAEs and sensor errors are < 48 ppm for all cases. This result suggests that the CFD model can provide insight into the vertical CO_2 concentration gradient and transport pattern in a ventilated room**.**

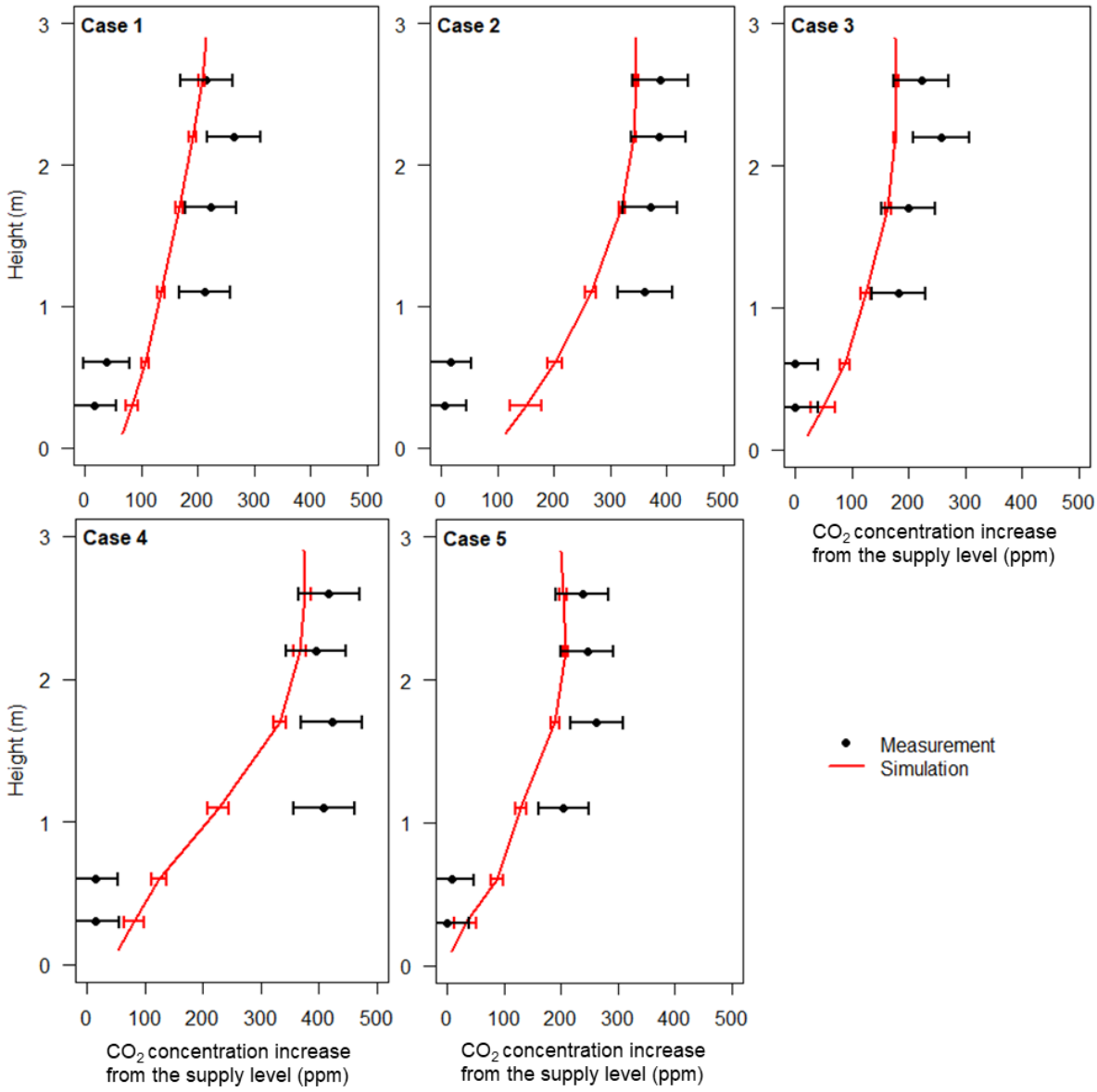

Figure 2. Comparison of the vertical CO_2 concentration profiles at six heights of 0.3, 0.6, 1.1, 1.7, 2.2, 2.6 m. Note that the horizontal axis is the CO_2 concentration increase from the supply.

https://doi.org/10.1016/j.enbuild.2019.109358
escholarship.org/uc/item/8n23p8c4

In addition to the experimental validation, we verified the mass and energy balances in the simulation domain for each case. Regarding the mass balance, the difference between inlet and outlet flow rates was maintained lower than 4×10^{-4} L/s. The simulated CO_2 concentration at the exhaust was within ±10 ppm of the theoretically calculated concentration from Eq. (3).

$$C(t_S) = \frac{G}{Q} \cdot (1 - e^{-\lambda t_S}) \cdot 10^6 + C_{out} \quad (3)$$

where $C(t_S)$ = exhaust CO_2 concentration (ppm)
G = CO_2 generation rate (m^3/h)
Q = outdoor air volumetric flow rate (m^3/h)
λ = air change rate (h^{-1})
t_S = solution time (h)
C_{out} = outdoor CO_2 concentration (ppm)

As for the energy balance, the difference between the total heat generation and heat removal was lower than 3×10^{-4} kW for the computation domain. The simulated exhaust air temperature was within ±0.14 °C different from the corresponding theoretically calculated temperature according to Eq. (4). These results further demonstrate the accuracy of the CFD simulations.

$$q = Q \cdot \rho \cdot c_p \cdot (T_e - T_s) / 3600 \quad (4)$$

where q = total heat load (kW)
Q = outdoor air volumetric flow rate (m^3/h)
ρ = air density (kg/m^3)
c_p = air specific heat (kJ/(kg·K))
T_e = air temperature at the room exhaust (°C)
T_s = supply air temperature (°C)

Note that considering it is more challenging to predict buoyancy-driven stratified airflow in displacement ventilation compared to the mixing airflow [30, 33, 35, 42], the experimental validation study focused on the scenarios with displacement ventilation. Although experimental validation was not performed for mixing ventilation cases, the simulation results were validated using the analytical solutions of the heat and mass balance in the simulation domain. The results show that differences between the simulations and analytical solutions at the room exhaust are < 10 ppm (1.5%) for CO_2 concentration and < 0.14 °C (0.5%) for air temperature.

2.2 Parametric analysis

The validated CFD model was used further for a parametric study that examined effects of three parameters: ventilation strategy (mixing vs. displacement), air change rate (2.5 and 5 h^{-1}), and occupancy level (one and five occupants) on the indoor CO_2 dispersion, which resulted in a total

of eight simulation scenarios as summarized in Table 2. When the room was occupied with five occupants, air change rates of 2.5 and 5 h^{-1} corresponded to air flow rates of 8 and 16 L/s·person, which were realistic for office spaces according to the minimum ventilation rate (4 L/s·person) defined by ANSI/ASHRAE standard 62.1 [18] and recommended ventilation rate (14 L/s·person) by CEN Standard EN 15251 [52]. For the scenarios with one occupant, the higher airflow rates of 38 and 76 L/s·person represented economizer ventilation system or dedicated outdoor air system.

Table 2. Test cases for parametric analyses (DV: displacement ventilation; MV: mixing ventilation).

Ventilation	Air change rate (h^{-1})	Air flow rate (L/s·person)	Occupant number	Steady–state CO_2 concentration (ppm)		Difference	
				Breathing zone	Exhaust	ppm	%
DV	2.5	38	1	599	648	50	8
DV	5	76		521	560	39	7
MV	2.5	38		615	647	31	5
MV	5	76		536	552	16	3
DV	2.5	8	5	1125	1353	228	20
DV	5	16		814	913	99	12
MV	2.5	8		1296	1349	53	4
MV	5	16		890	910	21	2

The CFD boundary conditions for displacement ventilation were the same as those of the validated model described in the Section 2.1.2. The inlet air velocity was 0.05 and 0.1 m/s for the case with air change rate of 2.5 and 5 h^{-1}, respectively. For the CFD models of mixing ventilation, the outdoor air was supplied through a 0.196 × 0.196 m large momentum diffuser at ceiling height (2.8 m from the floor) with the supply air temperature of 16 °C. The inlet air velocity was 1 and 2 m/s for the cases with air change rates of 2.5 and 5 h^{-1}, respectively. Figure S1 in Supporting Information shows the diffuser arrangement for mixing ventilation.

2.3 Evaluation of CO_2 sensor performance

To evaluate the effect of the sensor position on the sensing performance for the breathing zone CO_2 concentration, we simulated CO_2 release from occupants in the room and monitored the local concentrations at seven sampling locations (see Figure 3a) as follows:

1) Room exhaust (E) was monitored given that CO_2 sensors in individual rooms are commonly placed in the room exhaust or ventilation system return [7].

2) Four sampling points W1–W4 at four sidewalls at the height of 1.2 m, representing the wall-mounted sensors at breathing height for a sedentary occupant, i.e., 1.0 to 1.2 m above the floor. This sensor location is also common since the California Title 24 Standard [53] requires that CO_2 should be measured between 0.9 and 1.8 m above the floor. In fact, Mahyuddin and Awbi [26] reported that based on the database and questionnaires analysis, most researchers and building designers prefer to place sensors at the heights between 1.0 and 1.2 m.

3) Two sampling points D1 and D2 placed on the desk on the side and behind the monitor, respectively, representing the CO_2 sensors situated on the typical office desk.

Along with the CO_2 concentrations at seven sampling locations, we monitored the average CO_2 concentration within the breathing zone defined by ANSI/ASHRAE standard 62.1 [18], i.e. the space between planes 0.08 and 1.8 m above the floor and further than 0.6 m from the walls. The differences between the breathing zone concentration and local concentrations at sampling locations were estimated as the sensor errors for the DCV system, and the comparison results provided information on appropriate sensor positions to accurately represent the breathing zone CO_2 concentration.

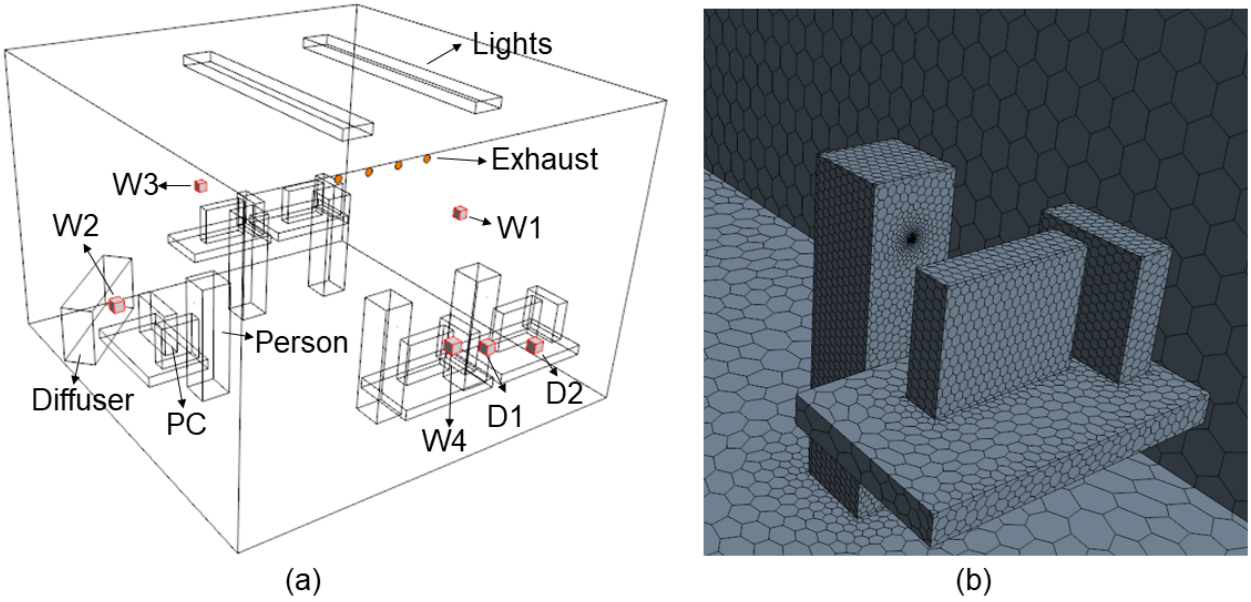

Figure 3. a) CFD geometry model; b) details of computational grid.

To evaluate the impact of sensor positioning on the outdoor air flow rate, we calculated the additional ventilation flow rates caused by the overestimation of the breathing zone CO_2 concentration for a variable air volume (VAV) air handling unit in a medium office building. The

calculation was based on the equilibrium carbon dioxide analysis approach where the outdoor air intake flow rate was calculated as follows [17]:

$$Q = n \cdot \frac{10^6 \cdot G}{(C_{in} - C_{out})} \quad (5)$$

where Q = outdoor air volumetric flow rate (m^3/h)
n = number of rooms
G = CO_2 generation rate (m^3/h)
C_{in} = equilibrium CO_2 concentration in the space (ppm)
C_{out} = outdoor CO_2 concentration, 400 ppm

The indoor CO_2 setpoint was set as 700 ppm since most of CO_2–based DCV for office buildings use the setpoint between 600 and 1000 ppm [7]. The flow rate was calculated assuming the air handling unit serves a single floor of the Department of Energy reference medium office building [54]. Furthermore, we calculated the additional power consumption associated with thermal conditioning of the extra outdoor air based on the enthalpy difference between outdoor air and the air leaving the cooling coil according to Eq. (6) [50].

$$q = Q \cdot \rho \cdot (h_1 - h_2) / 3600 \quad (6)$$

where q = total heat load (kW)
Q = outdoor air volumetric flow rate (m^3/h)
ρ = outdoor air density (kg/m^3)
h_1 = specific enthalpy of outdoor air (kJ/kg)
h_2 = specific enthalpy of air that leaves coil (kJ/kg)

Considering relatively large potential energy consumption for air conditioning in hot and humid climates, we carried out the calculations considering Miami, FL, USA as an example locale. The density and specific enthalpy of outdoor air were derived from the cooling design conditions for Miami [50]. The outdoor air density was 1.1 kg/m^3 and the enthalpy was 78 kJ/kg. The apparatus dew point of cooling coil was set to 8 °C and the specific enthalpy of leaving coil air was 25 kJ/kg.

Previous studies showed that 20–80% of total HVAC energy consumption is used for fan operation for large office buildings [55]. Therefore, we calculated the required fan power to move the additional air through the duct, heat exchanger and filter. The fan power was calculated using Eq. (7), which describes that fan power consumption P_f (kW) is proportional to the cube of the volumetric air flow rate [55].

$$P_f = a \cdot Q^3 \quad (7)$$

where a was the coefficient depending on the characteristics of fan and duct system, which was 1.36×10^{-12} kW/$(m^3/h)^3$ based on a previous study [56].

3. Results and discussion

The study results are organized into three sections. The first section presents CO_2 distribution patterns under varied building operating conditions. The second section compares CO_2 concentrations within the breathing zone and at the room exhaust under displacement and mixing ventilation. The last section evaluates the performance of CO_2 sensors at various locations and discusses how sensor position influences ventilation and energy performance of demand-controlled ventilation (DCV) system.

3.1 CO_2 concentration distribution

Figures 4a–d compare the horizontal CO_2 distributions at three different heights: 0.3, 1.2 and 2.4 m above the floor for the case with five occupants. Under displacement ventilation, the CO_2 concentration varies with height. With the air change rate of 2.5 h^{-1}, the average horizontal concentrations are about 700 ppm at 0.3 m, 1200 ppm at 1.2 m, and 1400 ppm at 2.4 m (see Figure 4a). In this case, the concentration difference between the floor and ceiling levels is about 800 ppm. Such large vertical variation is caused by the thermal plumes of occupants and computers that transport CO_2 to the upper zone.

When air change rate is increased to 5 h^{-1}, the average horizontal concentrations are 600 ppm at 0.3 m, 800 ppm at 1.2 m, and 900 ppm at 2.4 m (see Figure 4c). Although CO_2 stratification still exists, the concentration difference between the floor and ceiling level is about 400 ppm. This smaller vertical gradient is mainly due to the increased ventilation rate and a smaller residence time of CO_2 in the room.

Regarding mixing ventilation, CO_2 concentration distributions are relatively uniform compared to the displacement ventilation (see Figures 4b and 4d). In such cases, the supply air is introduced to the room with a high momentum and induces mixing of the room air. When the air change rate is 2.5 h^{-1}, the vertical concentration variation is lower than 150 ppm for the room, although high CO_2 concentrations exist in the vicinity of occupants under the effect of thermal plumes (see Figure 4b). With the air change rate of 5 h^{-1}, buoyancy-driven plumes are disrupted and the vertical concentration variation is lower than 50 ppm, indicating that the room air is nearly well-mixed (see Figure 4d). These results agree with the previous research of Mahyuddin and Awbi [25] that found 94 ppm of CO_2 concentration variation in a mixing ventilation system with a low air flow rate and more uniform CO_2 distributions with increased ventilation rates.

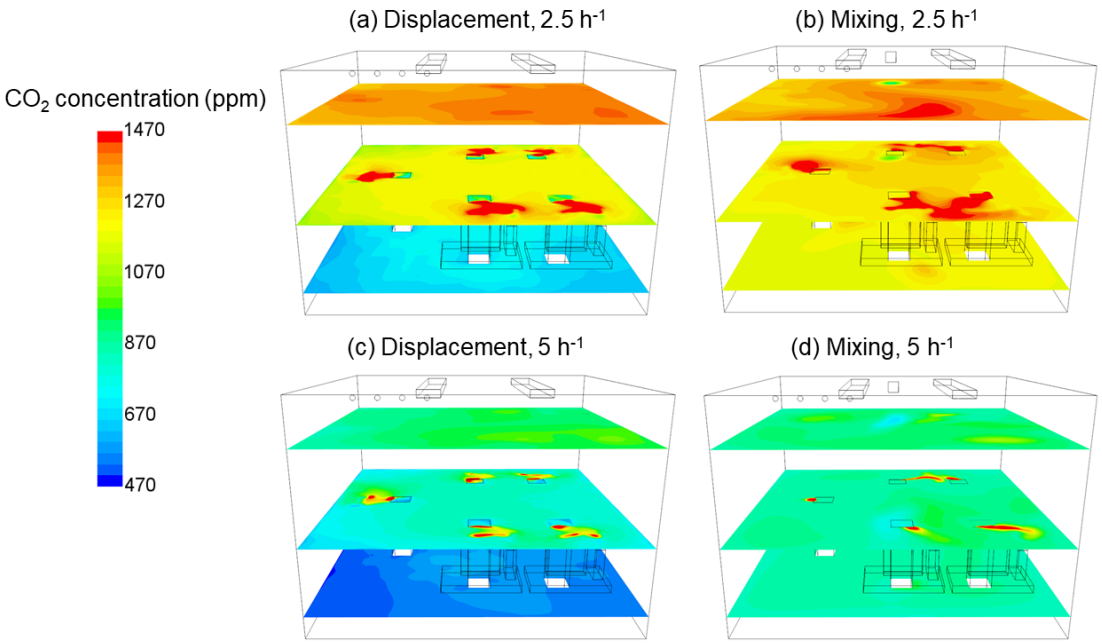

Figure 4. Distributions of CO_2 concentration on the horizontal sectional planes at three different heights of 0.3, 1.2 and 2.4 m with five occupants. (a) displacement ventilation with an air change rate of 2.5 h^{-1}; (b) mixing ventilation with an air change rate of 2.5 h^{-1}; (c) displacement ventilation with an air change rate of 5 h^{-1}; (d) mixing ventilation with an air change rate of 5 h^{-1}.

Figure 5 shows the vertical profiles of the horizontal surface-averaged CO_2 concentrations for displacement and mixing ventilation cases. Comparing the impact of the number of occupants, the vertical CO_2 gradient under displacement ventilation tends to be smaller with a lower occupancy (e.g., < 200 ppm with one occupant). Note that under displacement ventilation, the vertical CO_2 profiles exhibit two distinct zones: a lower transition zone where CO_2 concentration dramatically increases and an upper zone with a more uniform CO_2 concentration profile. It appears that the dividing height of the two zones varies with occupancy level in the room. For instance, the dividing height was about 1.5 m for the five occupant cases and 2.2 m for the one occupant cases in the present study. This phenomenon is in agreement with the realistic two-zone CO_2 distribution presented in REHVA Guidebook [57]. Several previous studies measured the vertical CO_2 profiles under displacement ventilation and reported the similar patterns [58-59]. Considering that the CO_2 concentration gradient is more pronounced in the lower transition zone and the dividing height varies with occupant density [58], the CO_2 sensors at the exhaust can yield more stable measurements than sensors at breathing height under displacement ventilation, especially when occupancy varies during different times of the day.

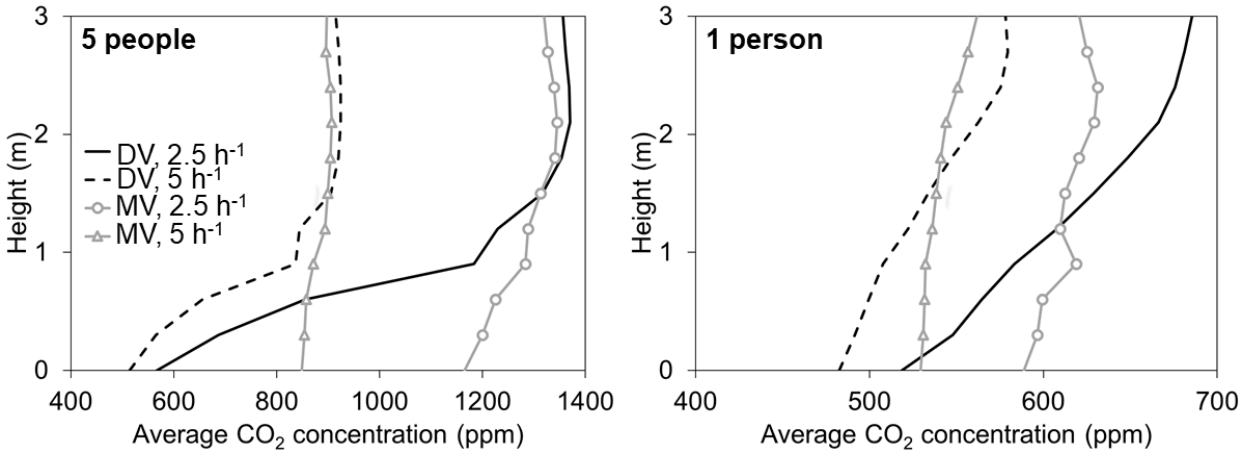

Figure 5. Vertical profiles of horizontal surface-averaged CO_2 concentrations with five occupants (left) and one occupant (right). Note that the horizontal-axis scale is 400–1400 ppm on the left figure while it is 400–700 ppm on the right figure.

3.2 Performance of exhaust CO_2 sensors under displacement and mixing ventilation

Knowing the vertical CO_2 distribution patterns depending on the ventilation strategy and occupancy level, Figures 6a–d compare the transient CO_2 concentration profiles at the room exhaust and in the breathing zone for the case with five occupants. The CO_2 concentration increases over time due to continuous CO_2 emission from the occupants until the steady–state is reached.

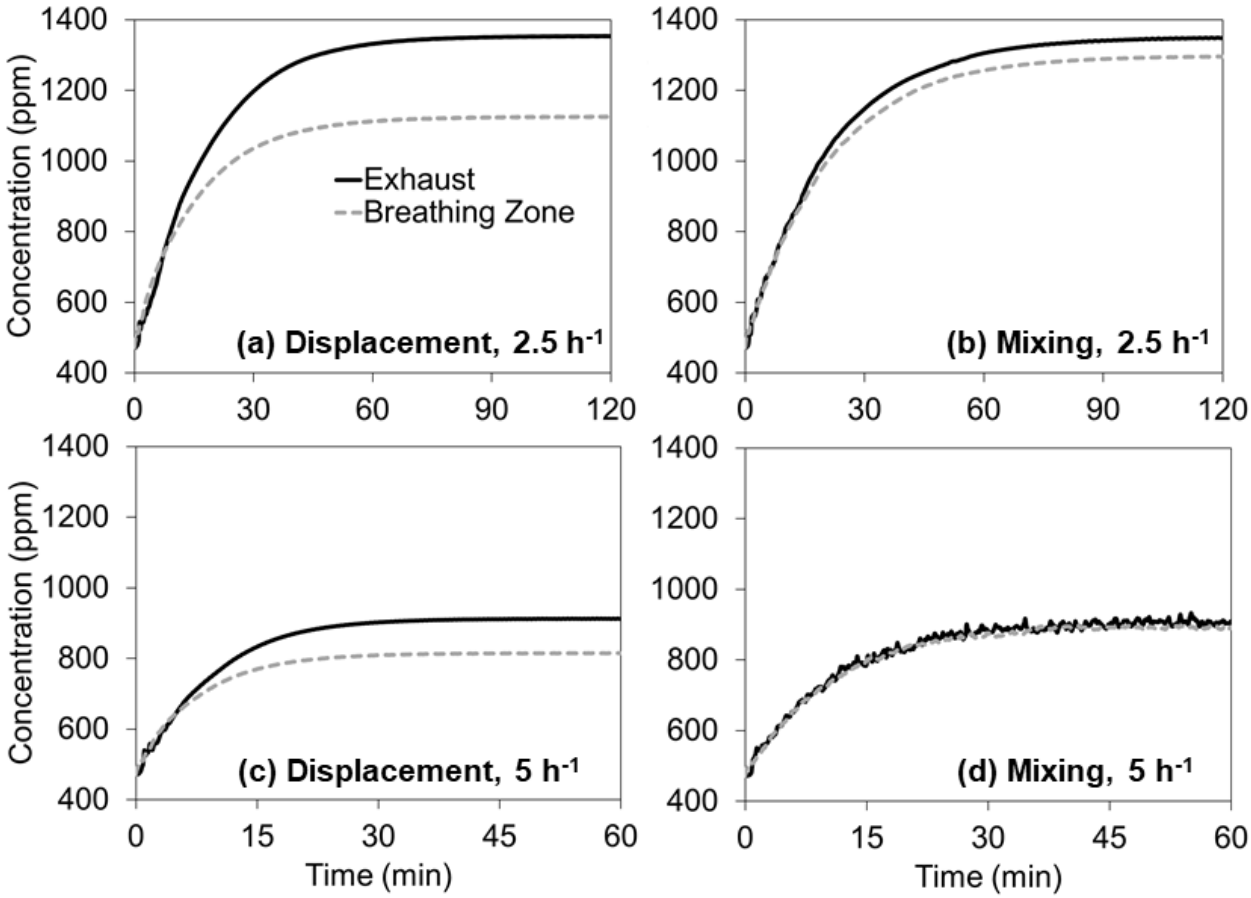

Figure 6. Transient CO_2 concentrations at the room exhaust and within the breathing zone in the case of five occupants in the room. (a) displacement ventilation with air change rate of 2.5 h^{-1}; (b) mixing ventilation with air change rate of 2.5 h^{-1}; (c) displacement ventilation with air change rate of 5 h^{-1}; (d) mixing ventilation with air change rate of 5 h^{-1}. Note that the x-axis scale of (c) and (d) is half that of (a) and (b).

With displacement ventilation and air change rate of 2.5 h^{-1} (Figure 6a), steady–state CO_2 concentration at the exhaust is about 230 ppm (20%) higher than the breathing zone. When the air change rate is 5 h^{-1}(Figure 6c), the exhaust concentration is about 100 ppm (12%) higher than the breathing zone. These differences are mainly attributed to CO_2 stratification in the displacement ventilated room (as described in Figure 4 and Figure 5). As for the mixing ventilation cases, the concentration differences between exhaust and the breathing zone over time are much smaller (53 ppm or 4% at 2.5 h^{-1} and 20 ppm or 2% at 5 h^{-1}) than those of displacement ventilation (see Figure 6b and 6d).

The demand controlled ventilation (DCV) strategy will only be effective when CO_2 sensors have a reasonable accuracy in practice [22]. CO_2 sensor readings higher than the actual breathing zone concentration can cause overventilation and lead to additional energy consumption, while the

lower readings result in insufficient ventilation and degraded indoor air quality in an occupied space [60]. ASTM E741-11 [61] states that when using a tracer gas to determine air change rates, the measured gas concentration shall differ by less than 10 % of the average concentration for the zone. The California Title 24 Standard [53] requires that the CO_2 sensors used for DCV must be factory-certified to have an accuracy within 75 ppm for the concentration range of 600-1000 ppm. In the present study, under displacement ventilation with five occupants in the room, the concentration difference between exhaust and the breathing zone exceeds 100 ppm with the percent difference larger than 10%. However, with mixing ventilation, the sensors placed at the room exhaust have discrepancies smaller than 55 ppm or 5%. The results suggest that for a room with mixing ventilation, the CO_2 sensors placed at the room exhaust can represent the breathing zone concentration with reasonable accuracy and meet the requirements of California Title 24 and ASTM E741. However, with displacement ventilation, the exhaust sensors can yield errors greater than the requirements for highly occupied spaces if the value is not adjusted considering the effect of stratification.

According to Table 2, the error of the exhaust sensor in predicting the breathing zone concentration tends to increase with lower ventilation rate and higher number of occupants. With only one occupant in the simulated room, the largest error under displacement ventilation with the air change rate of 2.5 h^{-1} is only 50 ppm (8%). With five occupants, the error goes up to 230 ppm (20%) under displacement ventilation and is only up to 53 ppm (4%) under mixing ventilation.

3.3 Effect of CO_2 sensor position

Figure 7 shows the deviations of the CO_2 concentration within the breathing zone from the concentrations at the seven different sensor locations.

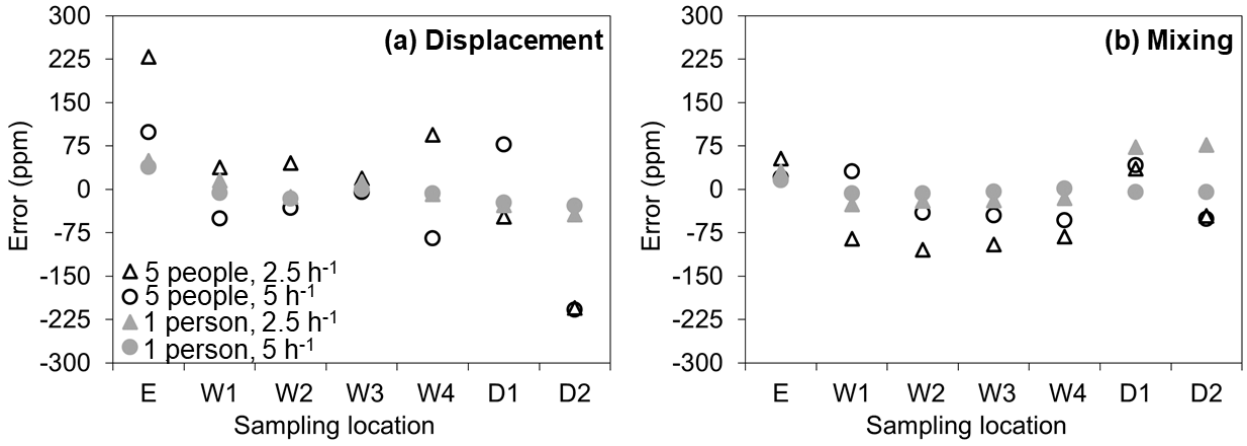

Figure 7. Sensor errors for seven locations under displacement (a) and mixing (b) ventilations.

Figure 7a presents that with five occupants under displacement ventilation at the air change rate of 2.5 h^{-1}, the wall–mounted sensors at 1.2 m height (W1–W4) have absolute errors ranging from

20 to 95 ppm (2 to 8% percent errors), which are much smaller than the exhaust sensor case (230 ppm or 20%). At the higher air change rate of 5 h^{-1}, the wall–mounted sensors have absolute errors ranging from 5 to 85 ppm (0.5 to 10%), while the exhaust sensor yields an error of 100 ppm (12%). These results reveal that the wall–mounted CO_2 sensors at breathing height can predict the breathing zone concentration with a higher accuracy compared to the exhaust sensor as long as the number of occupants (and all other heat gains) remains the same in the room until steady–state condition is reached. All four wall–mounted sensors yield percent errors within the accuracy of ASTM E741 requirements (10%), while three sensors (W1–W3) meet the requirement of California Title 24 (75 ppm).

The absolute errors for desk sensors D1 and D2 are up to 80 ppm and 210 ppm, respectively, with displacement ventilation. The results imply the desk sensors have unstable accuracies and can give significant errors because of the large CO_2 concentration gradient associated with the proximity to CO_2 emission. This trend agrees with a previous study by Rim and Novoselac [42] that reported highly non-uniform gaseous pollutant distributions near the human body due to natural convection flow near the occupant. These results show that the sensor location has a significant impact on the sensor error in the measurement of breathing zone CO_2 concentration under displacement ventilation and high occupancy. This is mainly due to the non-uniform and stratified CO_2 concentration as well as the thermal plumes around the heat sources as described in Figure 4 and 5. The cases with one occupant have the sensor errors less than 75 ppm for all sensor locations, implying smaller errors due to the sensor location in low occupancy conditions.

As for the mixing ventilation cases (see Figure 7b), the CO_2 concentrations at different locations are more uniform than those of displacement ventilation due to the air mixing in the room induced by the supply jet. All the sensors yield absolute errors < 105 ppm (8%). The results suggest that with mixing ventilation, the sensor location has less influence on the measurement of breathing zone CO_2 concentration than displacement ventilation case.

Figure 8 presents the additional ventilation flow rate and associated power consumption for the VAV air handling unit that serves a single floor of a medium office building due to the average CO_2 sensing error in measuring the breathing zone concentration as a function of the number of occupants. Section 3.2 depicts that CO_2 sensors placed at exhaust of the displacement ventilated room with five occupants results in overestimation of 230 ppm. As shown in Figure 8a, the average overestimation of 230 ppm can be translated to an additional flow rate of 20,000 L/s for the air handling unit that serves fifty rooms of the single floor. According to the ANSI/ASHRAE standard 62.1 [18] and CEN Standard EN 15251 [52], the recommended outdoor ventilation rates for the air handler is estimated to be 1000-3500 L/s, respectively. Comparing to these values, the additional ventilation flow rate of 20,000 L/s is 6-10 times greater. However, for the same condition, the maximum error (95 ppm) of wall-mounted sensors at breathing height is translated to an additional flow rate of 2800 L/s, which is about 86% smaller than the exhaust sensor case. Other wall mounted sensors yield only 400-1000 L/s of extra ventilation flow rates.

The increased outdoor airflow rate requires more energy consumptions for thermal conditioning as well as fan operation [4,12,55]. Figure 8b and 8c show the additional power consumptions for thermal conditioning and fan operation due to the CO_2 sensing error as a function of occupancy level in a hot and humid climate (Miami, FL). The average CO_2 overestimation of 230 ppm for the exhaust sensor can result in an additional power consumption of 1200 kW for thermal conditioning of the outdoor ventilation air in the air handling unit. For the same condition, the errors of wall-mounted sensors yield only 25–170 kW. The additional fan power with the average sensing error of 230 ppm with five occupants is estimated as 1100 kW, which is comparable to the power required for thermal conditioning. Since the required fan power for supplying air is proportional to the cube of the volumetric airflow rate [55], the additional fan energy consumption can be more significant with higher occupancy. For example, with 230 ppm error and ten occupants, the additional fan power is estimated to be 8600 kW. Therefore, even in climates that do not need much thermal conditioning, significant additional fan energy will be required to handle increased outdoor airflow rates due to CO_2 sensing error. These results suggest the importance of sensor positioning for CO_2–based DCV systems for achieving energy–efficient and healthy buildings.

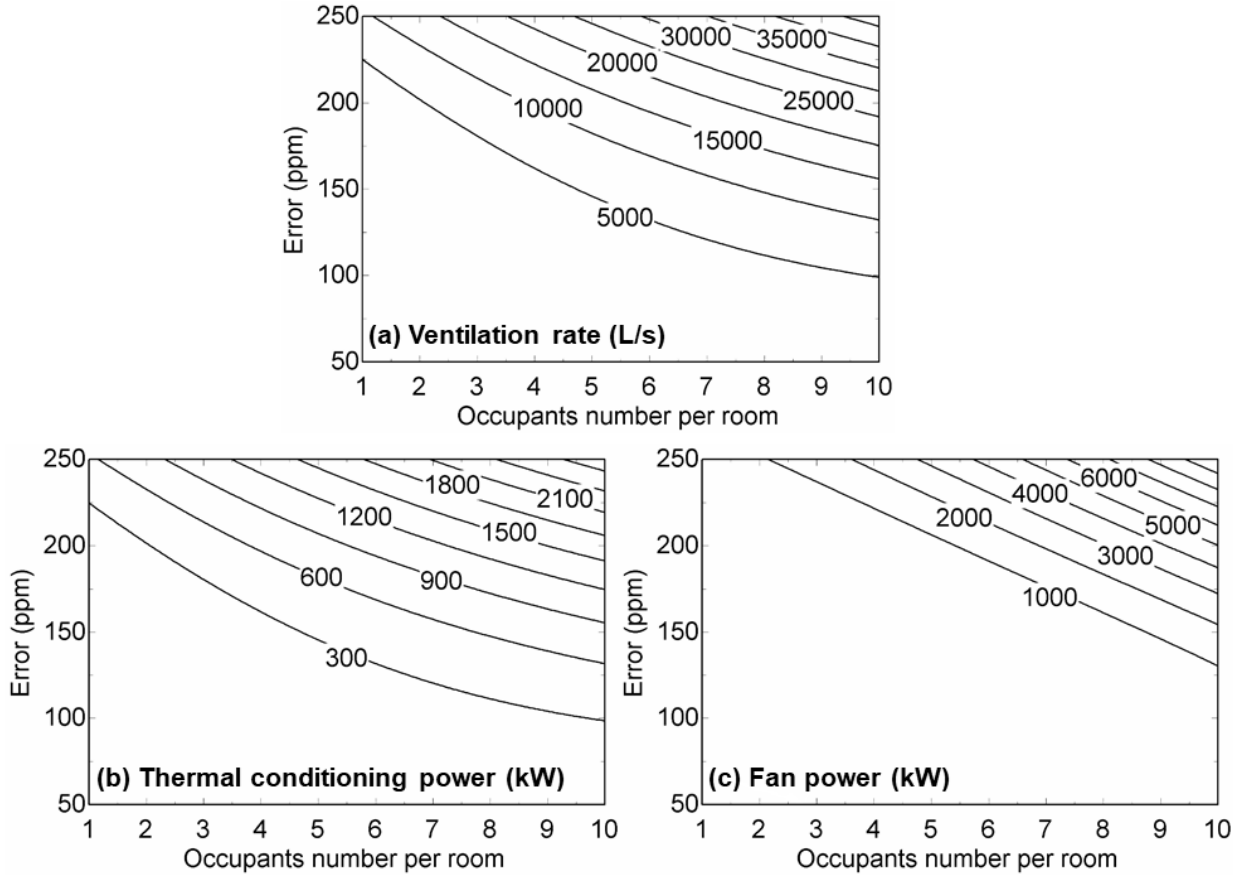

Figure 8. Additional ventilation rate (a), thermal conditioning power (b) and fan power (c) associated with the measurement error of CO_2 sensor as a function of the number of occupants per room.

https://doi.org/10.1016/j.enbuild.2019.109358
escholarship.org/uc/item/8n23p8c4

A few limitations of this study should be noted. While the present study reveals the effect of sensor position on the DCV performance in typical private or shared offices, future studies can perform the analysis for the different types of densely occupied spaces such as classrooms and auditoriums [62-63] given that high CO_2 concentrations and sensing errors can occur. In addition, the present study does not fully examine effects of asymmetric internal heat loads and interior partition walls on the non-uniform CO_2 concentrations in occupied spaces [35, 64-66]. Future studies are warranted to investigate how such conditions can contribute to the non-uniform CO_2 distributions and CO_2 sensing performance.

4. Conclusion

The present study employed experimentally validated Computational Fluid Dynamics simulations to examine the spatial distribution of CO_2 in a room while varying ventilation strategy, air change rate, and occupancy level. The study results provide information on the effect of sensor location on the ventilation and energy performance of CO_2–based demand controlled ventilation (DCV) system.

The study results show that ventilation strategy, occupant density, and air change rate have notable impacts on the CO_2 distribution in a room and accordingly the optimal sensor location. Under mixing ventilation, the sensor location has marginal influence on the measurement of breathing zone CO_2 concentration due to fairly uniform horizontal and vertical CO_2 distributions. In such cases, sensors placed at the room exhaust can meet the requirements of sensor accuracy in California Title 24 and ASTM E741.

However, displacement ventilation results in CO_2 stratification with two separated zones (lower transition zone and upper uniform zone). The dividing height of the two zones varies with the occupancy level and perhaps other parameters not explored in this study. A higher occupancy level with a lower air change rate can cause a larger vertical gradient of CO_2 concentration. The results also suggest that under displacement ventilation, placing CO_2 sensors on the desk or near occupants can yield significant errors due to the effect of occupant thermal plume and breathing. Wall–mounted CO_2 sensors at the breathing height result in less errors in predicting the breathing zone concentration than sensors near occupants or at the room exhaust, as long as the room is in steady–state condition. On the other hand, sensor readings at the breathing height may be unstable compared to the exhaust sensor because of a steep concentration gradient in the lower transition zone under the effect of varying occupancy.

The study results provide insights into the effect of CO_2 sensor location for the DCV system and highlight that DCV system design process should involve the understanding of optimal CO_2 sensor location based on ventilation and occupancy conditions. In general, CO_2 sensors located at the room exhaust can work well in predicting the breathing zone CO_2 concentration under mixing ventilation. However, under displacement ventilation, the exhaust sensors can overestimate the breathing zone concentration and result in additional energy consumption. Wall–mounted CO_2 sensors at breathing height yield relatively less errors in steady–state

condition, while the effect of varying occupancy should be considered. In addition, the results suggest that the CO_2 sensor location near occupants should be avoided. Future studies are warranted to develop quantitative relationships between CO_2 concentrations at the breathing height and at the exhaust for representative internal load conditions under displacement ventilation. Furthermore, it would be useful to investigate the feasibility of using such relationships in the CO_2–based displacement ventilation systems that serve densely occupied spaces.

Acknowledgements
This study is was funded by Penn State Institutes of Energy and the Environment Seed Grant (IEE) and ASHRAE (American Society of Heating, Refrigerating, and Air conditioning Engineers) Graduate Student Grant-in-aid (Gen Pei).

References

1. Seppänen, O. A., Fisk, W. J., & Mendell, M. J. (1999). Association of ventilation rates and CO_2 concentrations with health and other responses in commercial and institutional buildings. *Indoor air*, *9*(4), 226-252. https://doi.org/10.1111/j.1600-0668.1999.00003.x
2. Daisey, J. M., Angell, W. J., & Apte, M. G. (2003). Indoor air quality, ventilation and health symptoms in schools: an analysis of existing information. *Indoor air*, *13*(1), 53-64.
3. Sundell, J., Levin, H., Nazaroff, W. W., Cain, W. S., Fisk, W. J., Grimsrud, D. T., & Samet, J. M. (2011). Ventilation rates and health: multidisciplinary review of the scientific literature. *Indoor air*, *21*(3), 191-204. https://doi.org/10.1111/j.1600-0668.2010.00703.x
4. Rim, D., Schiavon, S., & Nazaroff, W. W. (2015). Energy and cost associated with ventilating office buildings in a tropical climate. *PLoS ONE 10(3): e0122310.* https://doi.org/10.1371/journal.pone.0122310
5. Sherman, M. H., & Matson, N. (1997). Residential ventilation and energy characteristics. *ASHRAE transactions*, *103*(1), 717-730.
6. Persily, A. K., & Emmerich, S. J. (2012). Indoor air quality in sustainable, energy efficient buildings. *Hvac&R Research*, *18*(1-2), 4-20. https://doi.org/10.1080/10789669.2011.592106
7. Emmerich, S. J., & Persily, A. K. (2001). State-of-the-art review of CO_2 demand controlled ventilation technology and application. NIST: National Institute of Standards and Technology.
8. Budaiwi, I. M., & Al−Homoud, M. S. (2001). Effect of ventilation strategies on air contaminant concentrations and energy consumption in buildings. *International journal of energy research*, *25*(12), 1073-1089. https://doi.org/10.1002/er.741
9. Faulkner, D., Fisk, W., & Walton, J. (1996). Energy savings in cleanrooms from demand-controlled filtration. *Journal of the IES*, *39*(6), 21-27. https://doi.org/10.17764/jiet.2.39.6.k8792h8164vk5218
10. Schibuola, L., Scarpa, M., & Tambani, C. (2016). Annual performance monitoring of a demand controlled ventilation system in a university library. *Energy Procedia*, *101*, 313-320.

https://doi.org/10.1016/j.egypro.2016.11.040
11. Shan, K., Sun, Y., Wang, S., & Yan, C. (2012). Development and In-situ validation of a multi-zone demand-controlled ventilation strategy using a limited number of sensors. *Building and environment*, *57*, 28-37. https://doi.org/10.1016/j.buildenv.2012.03.015
12. Fisk, W. J., & De Almeida, A. T. (1998). Sensor-based demand-controlled ventilation: a review. *Energy and buildings*, *29*(1), 35-45. https://doi.org/10.1016/S0378-7788(98)00029-2
13. Nassif, N., Kajl, S., & Sabourin, R. (2005). Ventilation control strategy using the supply CO2 concentration setpoint. *Hvac&R Research*, *11*(2), 239-262. https://doi.org/10.1080/10789669.2005.10391136
14. Sun, Z., Wang, S., & Ma, Z. (2011). In-situ implementation and validation of a CO2-based adaptive demand-controlled ventilation strategy in a multi-zone office building. *Building and Environment*, *46*(1), 124-133. https://doi.org/10.1016/j.buildenv.2010.07.008
15. Lee, S. C., & Chang, M. (1999). Indoor air quality investigations at five classrooms. *Indoor air*, *9*(2), 134-138. https://doi.org/10.1111/j.1600-0668.1999.t01-2-00008.x
16. ASTM. (2012). D6245-12: Standard guide for using indoor carbon dioxide concentrations to evaluate indoor air quality and ventilation. American Society for Testing and Materials.
17. Persily, A. K. (1997). Evaluating building IAQ and ventilation with indoor carbon dioxide. *ASHRAE transactions 103(2):*193–204.
18. ASHRAE. (2016). ANSI/ASHRAE Standard 62.1-2016: Ventilation for acceptable indoor air quality. Atlanta, GA, USA: American Society of Heating, Refrigeration, and Air Conditioning Engineers.
19. Schell, M.B., Turner, S.C. and Shim, R. O.. (1998). Application of CO_2−based Demand−controlled Ventilation using ASHRAE Standard 62: Optimizing Energy Use and Ventilation. *ASHRAE Transactions 104(2):*1231−1225.
20. Lu, T., Lü, X., & Viljanen, M. (2011). A novel and dynamic demand-controlled ventilation strategy for CO2 control and energy saving in buildings. *Energy and buildings*, *43*(9), 2499-2508. https://doi.org/10.1016/j.enbuild.2011.06.005
21. Liu, G., Dasu, A. R., & Zhang, J. (2012). Review of literature on terminal box control, occupancy sensing technology and multi-zone demand control ventilation (DCV) (No. PNNL-21281). Pacific Northwest National Lab.(PNNL), Richland, WA. https://doi.org/10.2172/1043117
22. Fisk, W.J., Sullivan, D.P., Faulkner, D., Eliseeva, E. (2010). CO_2 monitoring for demand controlled ventilation in commercial buildings. Lawrence Berkeley National Laboratory.
23. Stymne, H., Sandberg, M., & Mattsson, M. (1991). Dispersion pattern of contaminants in a displacement ventilated room-implications for demand control. *12th AIVC Conference,* Ottawa, Canada. 24-27 September, 1991.
24. Mundt, E. (1994). Contamination distribution in displacement ventilation—influence of disturbances. *Building and environment*, *29*(3), 311-317. https://doi.org/10.1016/0360-1323(94)90028-0

25. Mahyuddin, N., & Awbi, H. (2010). The spatial distribution of carbon dioxide in an environmental test chamber. *Building and Environment*, *45*(9), 1993-2001. https://doi.org/10.1016/j.buildenv.2010.02.001
26. Mahyuddin, N., & Awbi, H. (2012a). A review of CO_2 measurement procedures in ventilation research. *International Journal of Ventilation*, *10*(4), 353-370. https://doi.org/10.1080/14733315.2012.11683961
27. Mahyuddin, N., & Awbi, H. B. (2012b). Modelling the distribution of exhaled CO_2 in an environmental chamber. *10th International Conference on Healthy Buildings,* Brisbane, Australia. 8-12 July 2012
28. Bulińska, A., Popiołek, Z., & Buliński, Z. (2014). Experimentally validated CFD analysis on sampling region determination of average indoor carbon dioxide concentration in occupied space. *Building and Environment*, *72*, 319-331. https://doi.org/10.1016/j.buildenv.2013.11.001
29. Ning, M., Mengjie, S., Mingyin, C., Dongmei, P., & Shiming, D. (2016). Computational fluid dynamics (CFD) modelling of air flow field, mean age of air and CO_2 distributions inside a bedroom with different heights of conditioned air supply outlet. *Applied energy*, *164*, 906-915. https://doi.org/10.1016/j.apenergy.2015.10.096
30. Rim, D., & Novoselac, A. (2008). Transient simulation of airflow and pollutant dispersion under mixing flow and buoyancy driven flow regimes in residential buildings. *Ashrae Transactions*, *114*, 130-142.
31.Maldonado, E. A. B., & Woods, J. E. (1983). A method to select locations for indoor air quality sampling. *Building and Environment*, *18*(4), 171-180. https://doi.org/10.1016/0360-1323(83)90025-2
32. Chen, Q., & Srebric, J. (2002). A procedure for verification, validation, and reporting of indoor environment CFD analyses. *HVAC&R Research*, *8*(2), 201-216. https://doi.org/10.1080/10789669.2002.10391437
33. Shan, W., & Rim, D. (2018). Thermal and ventilation performance of combined passive chilled beam and displacement ventilation systems. *Energy and Buildings*, *158*, 466-475. https://doi.org/10.1016/j.enbuild.2017.10.010
34. Rim, D., Gall, E. T., Ananth, S., & Won, Y. (2018). Ozone reaction with human surfaces: Influences of surface reaction probability and indoor air flow condition. *Building and Environment*, *130*, 40-48. https://doi.org/10.1016/j.buildenv.2017.12.012
35. Ahn, H., Rim, D., & Lo, L. J. (2018). Ventilation and energy performance of partitioned indoor spaces under mixing and displacement ventilation. *Building Simulation*, *11*(3), 561-574. https://doi.org/10.1007/s12273-017-0410-z
36. Lakey, P.S., Morrison, G.C., Won, Y., Parry, K.M., von Domaros, M., Tobias, D.J., Rim, D. & Shiraiwa, M. (2019). The impact of clothing on ozone and squalene ozonolysis products in indoor environments. *Communications Chemistry*, *2*(1), 56. https://doi.org/10.1038/s42004-019-0159-7

37. Schiavon, S., Bauman, F., Tully, B., & Rimmer, J. (2012). Room air stratification in combined chilled ceiling and displacement ventilation systems. *HVAC&R Research*, *18*(1-2), 147-159. https://doi.org/10.1080/10789669.2011.592105
38. Comité Européen de Normalisation (CEN) (2004). CEN Standard DIN EN 14240: Ventilation for buildings - chilled ceilings - testing and rating, Brussels: CEN.
39. Srebric, J., & Chen, Q. (2002). An example of verification, validation, and reporting of indoor environment CFD analyses (RP-1133). *ASHRAE transactions*, *108*(2), 185-194.
40. Persily, A., & Jonge, L. (2017). Carbon dioxide generation rates for building occupants. *Indoor air*, *27*(5), 868-879. https://doi.org/10.1111/ina.12383
41. Deevy, M., & Gobeau, N. (2006). CFD modelling of benchmark test cases for a flow around a computer simulated person. HSL/2006/51. Health and Safety Laboratory, Buxton, UK.
42. Rim, D., & Novoselac, A. (2010). Occupational exposure to hazardous airborne pollutants: Effects of air mixing and source location. *Journal of occupational and environmental hygiene*, *7*(12), 683-692. https://doi.org/10.1080/15459624.2010.526894
43. Peric, M., & Ferguson, S. (2012). The advantage of polyhedral meshes. Technical report, CD-Adapco Group.
44. CD−adapco. (2012) User guide: STAR−CCM+. Version 12.02.011.
45. Menter, F. R. (1994). Two-equation eddy-viscosity turbulence models for engineering applications. *AIAA journal*, *32*(8), 1598-1605. https://doi.org/10.2514/3.12149
46. Argyropoulos, C. D., & Markatos, N. C. (2015). Recent advances on the numerical modelling of turbulent flows. *Applied Mathematical Modelling*, *39*(2), 693-732. https://doi.org/10.1016/j.apm.2014.07.001
47. Gilani, S., Montazeri, H., & Blocken, B. (2016). CFD simulation of stratified indoor environment in displacement ventilation: Validation and sensitivity analysis. *Building and Environment*, 95, 299-313. https://doi.org/10.1016/j.buildenv.2015.09.010
48. Versteeg, H. K., & Malalasekera, W. (2007). An introduction to computational fluid dynamics: the finite volume method. Longman Scientific and Technical.
49. Ferziger, J. H., & Peric, M. (2012). Computational methods for fluid dynamics. Springer Science & Business Media. Springer, Berlin.
50. ASHRAE. (2017). ASHRAE Handbook-Fundamentals. Atlanta, GA, USA: American Society of Heating, Refrigeration, and Air Conditioning Engineers.
51. Kobayashi, N., & Chen, Q. (2003). Floor-supply displacement ventilation in a small office. *Indoor and Built Environment*, *12*(4), 281-291. https://doi.org/10.1177/1420326X03035918
52. Comité Européen de Normalisation (CEN) (2007). CEN Standard EN 15251: Indoor environmental input parameters for design and assessment of energy performance of buildings addressing indoor air quality, thermal environment, lighting and acoustics, Brussels: CEN.
53. CEC. (2019). Building Energy Efficiency Standards for Residential and Nonresidential Buildings. California Energy Commission.

54.Deru, M., Field, K., Studer, D., Benne, K., Griffith, B., Torcellini, P., Liu, B., Halverson, M., Winiarski, D., Rosenberg, M. and Yazdanian, M. (2011). US Department of Energy commercial reference building models of the national building stock.
55.ASHRAE. (2012). ASHRAE Handbook-HVAC systems and equipment. Atlanta, GA, USA: American Society of Heating, Refrigeration, and Air Conditioning Engineers.
56.Hao, H., Lin, Y., Kowli, A. S., Barooah, P., & Meyn, S. (2014). Ancillary service to the grid through control of fans in commercial building HVAC systems. *IEEE Transactions on smart grid*, *5*(4), 2066-2074. https://doi.org/10.1109/TSG.2014.2322604
57.Skistad, H., Mundt, E., Nielsen, P. V., Hagström, K., & Railio, J. (2002). Displacement ventilation in non-industrial premises. 1st ed. REHVA Guidebook 1. Belgium: Federation of European Heating and Air-conditioning Associations.
58.Xu, M., Yamanaka, T., & Kotani, H. (2001). Vertical profiles of temperature and contaminant concentration in rooms ventilated by displacement with heat loss through room envelopes. *Indoor air*, *11*(2), 111-119. https://doi.org/10.1034/j.1600-0668.2001.110205.x
59.Kanaan, M., Ghaddar, N., & Ghali, K. (2010). Simplified model of contaminant dispersion in rooms conditioned by chilled-ceiling displacement ventilation system. *HVAC&R Research*, *16*(6), 765-783. https://doi.org/10.1080/10789669.2010.10390933
60.Dougan, D. S., & Damiano, L. (2004). CO_2-based demand control ventilation: Do risks outweigh potential rewards? *ASHRAE journal*, *46*(10), 47.
61.ASTM. (2011). E741-11. Standard test method for determining air change in a single zone by means of a tracer gas dilution. *American Society for Testing and Materials*.
62.Rim, D., Gall, E. T., Kim, J. B., & Bae, G. N. (2017). Particulate matter in urban nursery schools: A case study of Seoul, Korea during winter months. *Building and Environment*, *119*, 1-10. https://doi.org/10.1016/j.buildenv.2017.04.002
63.Kavgic, M., Mumovic, D., Stevanovic, Z., & Young, A. (2008). Analysis of thermal comfort and indoor air quality in a mechanically ventilated theatre. *Energy and Buildings*, *40*(7), 1334-1343. https://doi.org/10.1016/S0378-7788(01)00095-0
64.Lestinen, S., KilpelÄinen. S., Kosonen, R., Jokisalo, J., Koskela, H., Li, A. & Cao, G. (2019). Indoor airflow interactions with symmetrical and asymmetrical heat load distributions under diffuse ceiling ventilation. *Science and Technology for the Built Environment*. https://doi.org/10.1080/23744731.2019.1588029
65.Koskela, H., Häggblom, H., Kosonen, R., & Ruponen, M. (2010). Air distribution in office environment with asymmetric workstation layout using chilled beams. *Building and Environment*, *45*(9), 1923-1931. https://doi.org/10.1016/j.buildenv.2010.02.007
66.Huan, C., Wang, F. H., Lin, Z., Wu, X. Z., Ma, Z. J., Wang, Z. H., & Zhang, L. H. (2016). An experimental investigation into stratum ventilation for the cooling of an office with asymmetrically distributed heat gains. *Building and Environment*, *110*, 76-88. https://doi.org/10.1016/j.buildenv.2016.09.031

Supporting Information

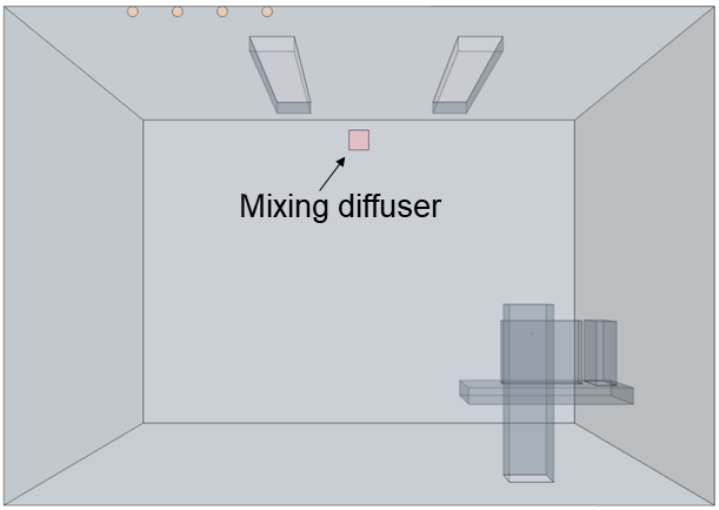

Figure S1. Arrangement of mixing diffuser.